


Benchmarking a boson sampler with Hamming nets

Iliia A. Iakovlev ^{1,2} Oleg M. Sotnikov ^{1,2} Ivan V. Dyakonov,³ Evgeniy O. Kiktenko ² Aleksey K. Fedorov ²
Stanislav S. Straupe,^{2,3} and Vladimir V. Mazurenko ^{1,2}

¹*Theoretical Physics and Applied Mathematics Department, Ural Federal University, Ekaterinburg 620002, Russia*

²*Russian Quantum Center, Skolkovo, Moscow 121205, Russia*

³*Quantum Technology Centre and Faculty of Physics, M. V. Lomonosov Moscow State University, Moscow 119991, Russia*



(Received 14 June 2023; accepted 22 November 2023; published 19 December 2023)

Analyzing the properties of complex quantum systems is crucial for further development of quantum devices, yet this task is typically challenging and demanding with respect to the required amount of measurements. Special attention to this problem appears within the context of characterizing outcomes of noisy intermediate-scale quantum devices, which produce quantum states with specific properties so that it is expected to be hard to simulate such states using classical resources. In this work, we address the problem of characterization of a boson sampling device, which uses the interference of input photons to produce samples of nontrivial probability distributions that at certain condition are hard to obtain classically. For realistic experimental conditions the problem is to probe multiphoton interference with a limited number of the measurement outcomes without collisions and repetitions. By constructing networks on the measurement outcomes, we demonstrate the possibility to discriminate between regimes of indistinguishable and distinguishable bosons by quantifying the structures of the corresponding networks. Based on this, we propose a machine-learning-based protocol to benchmark a boson sampler with unknown scattering matrix. Notably, the protocol works in the most challenging regimes of having a very limited number of bitstrings without collisions and repetitions. As we expect, our framework can be directly applied for characterizing boson sampling devices that are currently available in experiments.

DOI: [10.1103/PhysRevA.108.062420](https://doi.org/10.1103/PhysRevA.108.062420)

I. INTRODUCTION

The idea behind quantum computing is to manipulate complex (entangled, many-body) quantum states to solve computational problems [1–3]. Certain quantum algorithms use a feature of a possibility to efficiently check the correctness of the obtained results, for example, as it takes place for the Shor’s factorization algorithm [4]. In a general case, however, the problem of characterization and verification of quantum states that are produced by quantum computing devices is highly nontrivial, yet it is essential to understand whereas the quantum devices work correctly. This task becomes even more challenging taking into account the fact that currently developed quantum processors are highly affected by decoherence, so they belong to the class of noisy intermediate-scale quantum (NISQ) devices. A celebrated example is a seemingly unresolvable problem of sampling the output of a pseudorandom 53-qubit circuit performed by the Google team [5] with the Sycamore processor, which is exponentially more difficult to do with classical computing. This breakthrough study stimulated the development of the methods not only for efficient simulating large-scale quantum wave function on classical devices [6–11], but also approaches for distinguishing quantum states delocalized in the Hilbert space from each other with a very limited number of measurements [12,13]. Recent random circuit sampling experiments [14] with 70 qubits defined a new boundary for demonstrating quantum advantage.

In addition to the gate-based model of quantum computing, remarkable progress with the developing of boson sampling

(BS) [15–17] has been performed [18] (starting by first experimental realizations [19–21]). Currently, BS represents a popular quantum playground for testing novel approaches [22–26] where one faces a certification problem for a photon device with exponentially large output state space in the absence of a classical counterpart imitated with a classical computer [27,28]. More specifically, for a given device that takes n photons as an input and allocates them over m output modes according to some probability distribution function, one should be able to certify that the outcome data arise from indistinguishable photons with a limited number of measurements. Recent experiments on large-scale boson sampling have been used to demonstrate quantum computational advantage [29–32]. The certification of a boson sampler generally assumes, first, unambiguously distinguishing it from a classical device that generates outcomes according to a distribution, for instance, a uniform one. Moreover, a related problem is to define whether given sets of samples were drawn from the same boson sampler or different ones [22]. Finally, from practical perspective recognizing the regimes of indistinguishable bosons to distinguishable ones, when performing a limited number of experiments with a boson sampler is also of great importance.

There are, generally speaking, two widely used strategies for solving the problem of verification of a boson sampler. The first one assumes that one exploits an insider information on the boson sampler in question. For instance, it could be details of a scattering matrix U describing the connection between input and output modes [33–36]. The existence of a trusted boson sampler that is assumed in some studies [37]

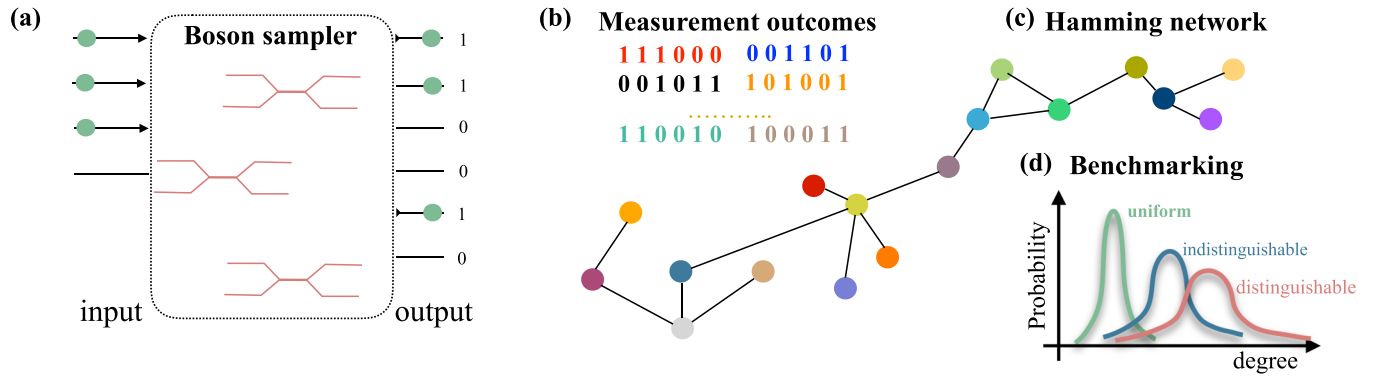


FIG. 1. Protocol for constructing a Hamming network and certification of a boson sampler. (a) Schematic representation of the boson sampler that takes three photons as input and distributes them over output modes according to some probability distribution function. (b) A limited set of outcomes (bitstrings) without repetitions and collisions as obtained from the boson sampler. (c) Construction of the network in which each node corresponds to the specific bitstring. If the Hamming distance between two bitstrings is smaller than or equal to the chosen cutoff radius R , then the corresponding nodes are connected. For each node the total number of links (degree) is calculated. (d) Distribution of the nodes (bitstrings) with respect to their degree allows discriminating between sets of uniform, distinguishable, and indistinguishable boson bitstrings.

can also considerably facilitate the validation of a photonic device with different clustering techniques. The second class of approaches for certifying boson samplers fully relies on the analysis of the measurement outcomes. For instance, the statistical benchmarking proposed in Ref. [23] is based on the calculation of pair correlation functions for all possible output modes combinations. While, theoretically, these correlators allow one to probe many-particle interference, the practical realization of such a benchmarking requires some experimental efforts in performing numerous measurements for all possible inputs and should be verified in each case.

The complexity of the boson sampler certification [31,38] suggests to make use of the entire arsenal of available methods, including those from completely different fields of research dealing with problem of analyzing complex processes. For instance, a fresh look at the problem can be taken with machine learning (ML) techniques including clustering methods [22,37,39], the combination of the low-dimensional representation and convolutional neural network [40], or others. While the main focus in these ML-based studies is on the Hamming distance (or L_1 norm) between bitstrings $b_i = (b_i^1, \dots, b_i^m)$ and $b_j = (b_j^1, \dots, b_j^m)$ that is defined as $\mathcal{D}_{ij} = \sum_{k=1}^m |b_i^k - b_j^k|$, as it has been shown, taking into account collisions as well as bitstrings statistics also plays an important role in validating boson sampler. Remarkably, discriminating sets of boson sampler outcomes without both collisions of photons and repetitions of events has not been demonstrated up to date, which actually corresponds to a typical experimental situation.

In this work, we propose and demonstrate a protocol for retrieving meaningful information about a photon interferometer, which can be extracted even when collision- and repetition-free sets of boson sampler outcomes are only available. For this purpose, we use the concept of the Hamming network recently introduced in Ref. [13] for the analysis of the complexity of the quantum wave functions and detecting quantum phase transitions. Specifically, we apply it to explore the structure of links in the Hamming network constructed on the basis of the measurement outcomes of a boson sampler

[see, Figs. 1(a) and 1(b)]. Each BS event is associated with a colored node in the Hamming network. Since there are no repetitions of the bitstrings, there are no nodes of the same color in Fig. 1(c). Having chosen a cutoff radius R that can be in the range between minimal and maximal bitstring distances within the entire ensemble of outcomes, one compares it to the Hamming distances of individual bitstring pairs. If $R \geq \mathcal{D}_{ij}$, we connect the i th and j th events with a link. According to the network theory, the amount of connections a particular node has is called its degree. Computing the statistics over the degrees [Fig. 1(d)] in the network constructed for a given set of measurements outcomes allows characterization of the boson sampler in the situation of information scarcity. As is shown below, one can discriminate between uniform and nonuniform samplers, as well as the distinguishable and indistinguishable regimes of BS.

II. RESULTS

A. Constructing Hamming networks

We start our consideration with constructing Hamming networks for the collision-free sets of bitstrings that were generated with loading n photons into the boson samplers of $m = n^2$ output modes, where $n = 4, 5, 6$, and 7 . According to Ref. [15] it is believed that such a quadratic dependence of modes number on n corresponds to the lower bound for demonstrating quantum advantage with boson sampling. In these BS settings the total number of the unique collision-free outcomes is defined as C_m^n and equal to 1820 ($n = 4$), 53 130 ($n = 5$), 1 947 792 ($n = 6$) and 85 900 584 ($n = 7$). By “collision-free set” we mean that all n photons are detected in distinct output modes. This regime is consistent with commonly used photodetectors that do not allow for photon number discrimination. From the point of view of real boson sampling experiments the considered configurations are realistic and imitate characteristics of the state-of-the-art devices [34,41,42]. A detailed technical information concerning the boson sampler simulator we use is given in Appendix A. We would like to stress that each outcome (bitstring) is

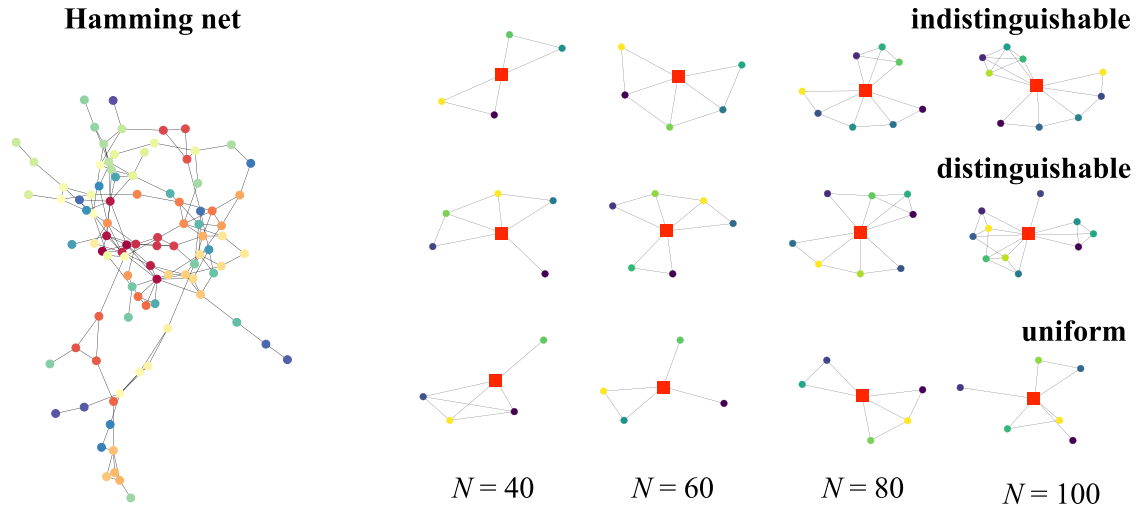


FIG. 2. (Left) Example of the Hamming network constructed for 100 outcomes taken from the boson sampler with four bosons and 16 output modes in the regime of indistinguishable particles. The cutoff radius R is equal to 2. (Right) Fragments of the Hamming networks that contain nodes (red square) with the largest degree. These networks were constructed with $N = 40, 60, 80,$ and 100 bitstrings from indistinguishable (top row), distinguishable (middle row), and uniform (bottom row) photons sources.

unique within the particular set, which excludes using the outcome's statistics for recognizing the many-particle interference regime realized in BS. It makes the approaches relying on the choice of the states with highest probability [22,37] out of game and strongly motivates to employing methods [13] that can reveal hidden dependencies, structures, and correlations in a limited amount of data.

The main parameter when constructing the network for a set of outcomes is the cutoff radius R that defines the particular structure of the Hamming network. Since all the bitstrings we collect have the same number of “1” bits the minimal difference in the Hamming distance \mathcal{D}_{ij} between two arbitrary chosen bitstrings is equal to 2, which is the minimal step for the cutoff radius change. In Fig. 2 we give an example of such a net constructed with $R = 2$ for which all the links have the same weight. In other words, within our approach to differentiate the photon sources we will only use the information about number of degrees. One can see that, in the case of the small $R = 2$, there are many nodes with a few links, which can be explained by the small number of bitstrings in the sample and a nonuniform distribution of the corresponding bitstrings over state space. Visualization of the network's fragments is shown in Fig. 2 and constructed with minimal cutoff radius, and small sets of bitstrings reveal a difference in change of the largest presented degree depending on the size of the bitstrings set for uniform and nonuniform samplers. In the case of the nets constructed with uniform distribution this quantity increases more slowly than for distinguishable and indistinguishable ones. At the same time, by these fragments we cannot discriminate the distinguishable and indistinguishable photons sources. In both cases the graphs obtained for the same number of bitstrings look similar.

Such a structural difference between networks constructed with uniform and nonuniform samples becomes more evident when analyzing the probability distributions P_k of the network nodes with respect to their degree k . One can think about P_k as a probability that a random node in the Hamming net has exactly k neighbors. The results obtained for individual

samples of 512 bitstrings and presented in Fig. 3(a) demonstrate different locations of the means of these distributions. This paves the way for benchmarking outcomes from a nonuniform sampler in a fully unsupervised manner. More specifically, for a given set of bitstrings obtained from an unknown sampler we are able to generate the same number of bitstrings distributed uniformly, which can be done efficiently with a classical computer. Then, one constructs networks with bitstrings from unknown device and uniform sampler. By comparing the means and standard deviations of the resulting probability distribution functions one can make the conclusion whether the initial set of bitstrings was generated with a uniform or nonuniform unknown sampler. The validity of the proposed certification procedure is confirmed by the results that were averaged over 512 samples taken from the same interferometer [Fig. 3(b)] and those averaged over 100 independent interferometers [Fig. 3(c)]. In all cases the difference in the distribution properties between the uniform and nonuniform samplers is robust.

If one gets information about the scattering matrix U of the device to be certified, there are efficient algorithms such as the test of Aaronson and Arkhipov [43] that can validate a boson sampler against uniform on the basis of several outcomes. Importantly, the practical implementation of this test does not assume the calculation of any permanent. In the cases when the details of the multiparticle interferometer are unknown, one can make use of a kind of clustering algorithm. For instance, to characterize a boson device, a bubble clustering protocol [22] proposed by Wang and Duan determines the structure of the bit-string sample by utilizing the frequency of generating individual outcomes. Our approach is different since constructing Hamming nets to certify a BS device excludes repetitions in bit-string samples.

While recognizing uniform samplers is straightforward with Hamming nets, the certification of distinguishable and indistinguishable BS regimes is found to be a more challenging task. As follows from Figs. 3(b) and 3(c), the averaging over samples and over scattering matrices leads to a strong

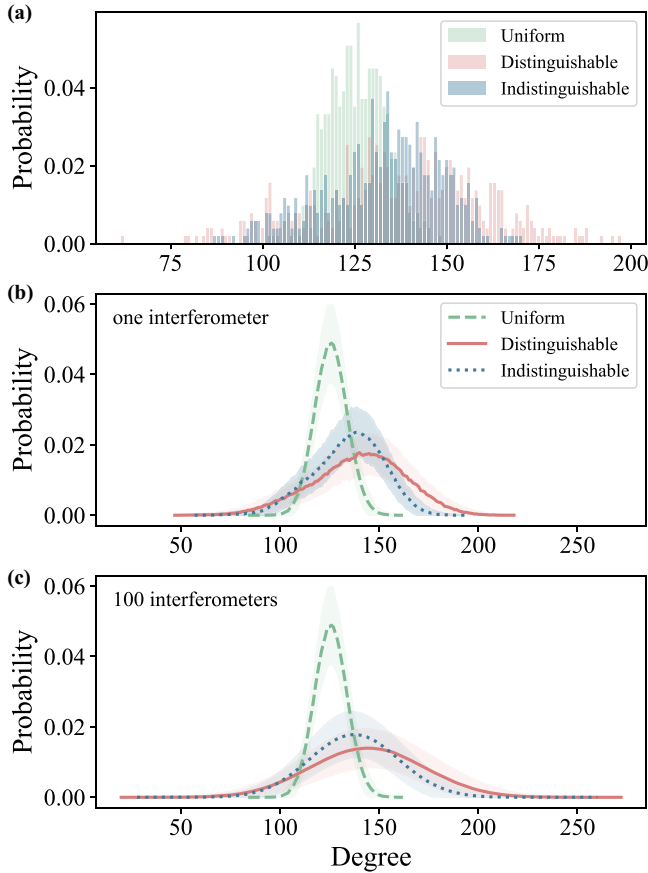


FIG. 3. Comparison of the degree distributions estimated from the Hamming nets that were constructed with uniform (green), distinguishable (red), and indistinguishable (blue) samplers outcomes. These results were obtained for boson sampler with 16 modes and four photons and cutoff radius $R = 4$. (a) Comparison of the distributions on the level of single sample of 512 bitstrings. (b) Data averaged over 512 samples each containing 512 bitstrings obtained from the same interferometer. (c) Results averaged over 100 interferometers. Data for each interferometer were averaged over 512 samples with size $N = 512$.

dispersion (colored regions) of the probabilities' functions, P_k^D (for distinguishable particles) and P_k^I (for indistinguishable particles). In other words, a sampler can give a distribution of the nodes that will strongly differ from the mean probability profiles denoted with lines in Fig. 3(c). Although there are some differences in the mean and standard deviation values between the averaged distinguishable and indistinguishable data [Fig. 3(c)], such differences are too small to be used by a researcher for a manual benchmarking of a boson sampler. It motivates us to develop a machine learning protocol for certifying boson samplers as described in the next section.

B. Machine learning BS regimes

The theoretical description of a system or a process with a limited number of observations available for a researcher is a standard task in science that may arise in various fields. In physics, classifying different types of Brownian motion with short trajectories [44,45], constructing a phase diagram on

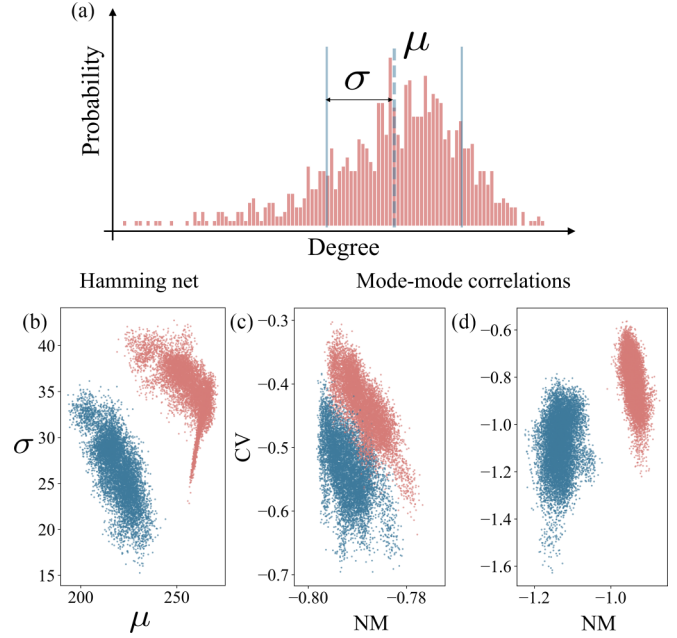


FIG. 4. (a) Schematic representation of the P_k distribution obtained using $N = 1024$ bitstrings at $R = 6$. (b)–(d) Low-dimensional visualisations of the configurations taken from the training sets for $n = 4$ bosons and $m = 16$ output modes, $N = 1024$, and the cutoff radius of 4. Red (light gray) and blue (dark gray) clouds correspond to distinguishable and indistinguishable particles, respectively. Features were taken from (b) the Hamming network and (c,d) correlation functions approaches. (d) The last data set includes collisions and repetitions. NM and CV denote the normalized mean and coefficient of variation, which are the features introduced in Ref. [23] within the mode-mode correlation function approach.

the basis of limited number of system's snapshots [46,47], approximating the ground state of a quantum Hamiltonian on a quantum computer [48], and certifying a quantum state on a quantum device by means of a few measurements [12] represent only a few notable examples of problems among many others. Remarkably, in these and other cases machine learning (ML) has turned out to be a very valuable alternative to standard techniques and advancing the corresponding fields of research. In this sense, the boson sampling is no exception and there are various machine learning based schemes for benchmarking boson devices. They include basic clustering ML algorithms [49] and neural network approaches [40] as well.

In our case discriminating devices with distinguishable and indistinguishable photons on the level of the Hamming networks can be also advanced with basic machine learning. To show that, we first perform a feature selection procedure. We find out that the most reliable features are two first moments of the P_k distributions for such intermediate cutoff radii R for which P_k is Gaussian-like and has both left and right sides [Fig. 4(a)]. Namely, we use $R = \{2, 4, 6\}$, $R = \{2, 4, 6, 8\}$, $R = \{4, 6, 8, 10\}$, and $R = \{6, 8, 10, 12\}$ for the samplers with $n = 4, 5, 6$, and 7 photons, respectively. More details on the radii choice are given Appendix B. By the example of the standard deviation and mean features presented in Fig. 4(b) one can see that the clouds formed from distinguishable and indis-

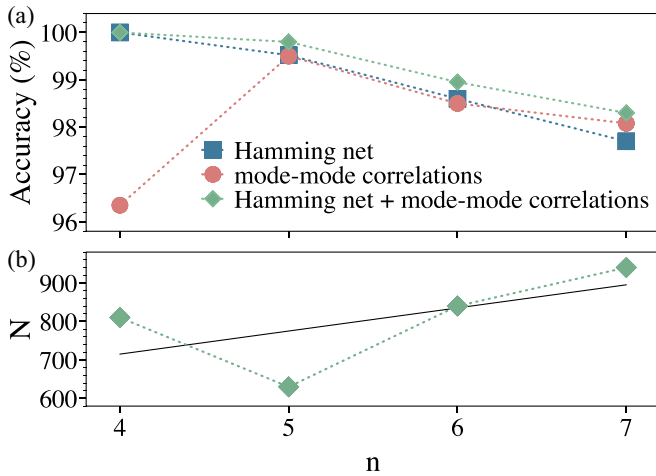


FIG. 5. Machine learning certification of boson samplers. (a) Accuracy of the logistic regression model on the testing data assessed on the unseen U matrices. The results are obtained using $N = 1024$ bitstrings in each sample. The error bars are smaller than the symbol size. (b) Dependence of the number of unique bitstrings N required to reach the accuracy $\sim 98\%$ on n . The machine learning algorithms here were trained on the features extracted from both Hamming net and mode-mode correlation functions. The amount of output modes is equal to $m = n^2$.

tinguishable outcomes are well separated for $n = 4$, which, as we will show below, provides a high accuracy in classification with ML.

At this stage, it is important to recall other quantities that are based on a mode-mode correlation function used in the previous theoretical [23,24,50] and experimental [31] works for benchmarking an indistinguishable sampler against a distinguishable one. Such correlation functions are defined as $C_{ij} = \langle n_i n_j \rangle - \langle n_i \rangle \langle n_j \rangle$, where n_i is the photon number in the i th mode. The features (normalized mean, coefficient of variation, skewness) extracted from distribution of the calculated C_{ij} allow discriminating among different samplers. As it follows from Fig. 4(c) our consideration challenges the previous results since the clouds formed by different samplers overlap in the feature space for bitstring sets subjected to additional selection. Comparison of Figs. 4(c) and 4(d) clearly shows that the outcomes' repetitions and collision events play a crucial role in forming well-separated clouds on the level of features. Thus, the regime without collisions and repetitions for $n = 4$ we explore in this work is of particular difficulty.

Since separating clouds in the feature plane is a kind of trade-off in our choice of the bitstring number in the sample with respect to the total size of the state space, it becomes important to implement the machine learning to control the classification quality for boson samplers with $n > 4$. Among the basic ML methods we tested (see Appendix C for more details) the best benchmarking results on scattering matrices unseen during the training stage were achieved with logistic regression (LR). From Fig. 5(a) one can see that the accuracy of the classification based on the Hamming net features gradually degrades as the number of bosons increases. For instance, in the case of $n = 7$ it is about 97.7% [blue squares

in Fig. 5(a)], which clearly indicates the smallness of the sample size ($N = 1024$) with respect to the total state space dimension (85 900 584).

In turn, the ML models based on mode-mode correlations demonstrate a considerable enhancement of the classification accuracy for $n = 5$ in comparison with $n = 4$. It can be explained by a larger effective separation of the centers of the clouds in low-dimensional representation of the data for distinguishable and indistinguishable particles. Nevertheless, the fact that there is the deviation from the ideal 100% certification of the particle type evidences nonzero overlap of the corresponding clouds. Figure 5(a) shows ML accuracy for mode-mode correlators that behaves similarly to that obtained with Hamming net data for $n > 4$. It has to be stressed one more time that the previous works based on the calculation of the mode-mode correlation functions did not develop an intuition about the performance of this approach in the case of the collision-free and repetition-free regimes and for the BS setting with $m = n^2$ dependence, which is one of the goals of this work.

Importantly, both the Hamming nets features and mode-mode correlation features are not correlated by the construction. This fact means that these features can be combined to achieve better performance in distinguishing boson samplers with machine learning. Indeed, in this case the resulting ML accuracy increases to $\sim 98.3\%$ for $n = 7$ [green diamonds in Fig. 5(a)]. These ML results clearly show that accurate benchmarking of unknown boson samplers is possible with a very limited number of bitstrings without collisions and repetitions.

Another important question is how the amount of unique bitstrings required to achieve certain accuracy scales with n . As can be seen from Fig. 5(b) N grows rather linearly and the obtained values are experimentally reachable which indicates the viability of the proposed approach. Here we fix the accuracy to be $\sim 98\%$. The reason why the BS with $n = 5$ requires less bitstrings to reach the same accuracy can be explained in the following way. On the one hand, it has more output modes and therefore more degrees of freedom than the BS with $n = 4$, which increase the difference in statistics of the considered regimes. On the other hand, the used N covers the larger portion of the entire basis than in the case of $n \geq 6$.

C. Three distinct measures of BS complexity

Characterizing photon interferometry is closely related to the problem of describing the sampling complexity. Traditionally, the main focus is on an exponential separation between quantum and classical sampling times, which is considered to be one of the important examples for demonstrating the quantum advantage. However, this is only one of the possible measures of how hard it is to create a sample with a given boson device (computational complexity). A detailed comparison of the distinguishable and indistinguishable bitstrings sources can enrich our understanding not only in terms of sampling complexity, but also in relation to the structure of the generated data, the quantification of information content, and others. In fact, there are more than 42 different measures [51,52] of the complexity that can be potentially used to characterize a system.

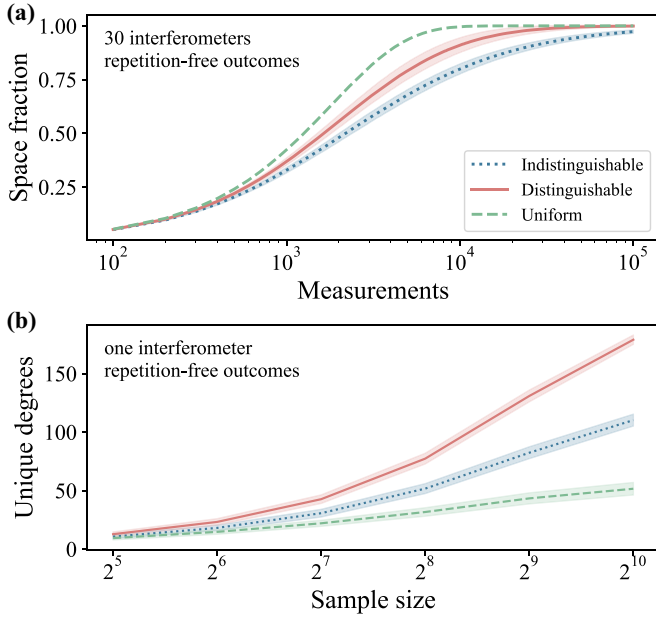


FIG. 6. Boson sampler complexity measures we analyze in this work. (a) Fraction of the states from the Hilbert space as function of performed measurements for uniform and boson sampler with 16 modes and four photons in regimes of distinguishable and indistinguishable photons. Curves for the boson sampler were averaged over 30 scattering matrices. (b) Unique degrees count of the sampler network graphs for distinct cutoff radius $R = 4$.

In this work, we propose three different measures to discriminate outcomes of the boson samplers with respect to the time computational complexity, complexity of the data structure, and complexity of describing the information content. The first one can be analyzed by the example of Fig. 6(a) that shows the difference between distinguishable and indistinguishable samplers in a fraction of the state space that is captured when performing a different number of measurements. One can see that it is more difficult to collect unique bitstrings in the case of an indistinguishable sampler than a distinguishable one with the same number of measurements. The largest difference is observed for 10^4 measurements. It can be understood from the fact that the probability distribution of the distinguishable bitstrings is closer to uniform than the indistinguishable one.

The second complexity measure that provides a robust quantitative characterization and discrimination of the constructed networks with respect to their structure is the number of the unique degrees of the network. By this we mean the number of classes in which each node has the same degree. In Fig. 6(b) we compare the dependencies of the number of the unique degrees on the sample size for distinguishable, uniform, and indistinguishable particles. These results evidence that, for a given scattering matrix, a robust discrimination of the multiphoton regimes can be fulfilled at the cutoff radius $R = 4$ for the samples that are characterized by minimal sizes of 2^7 , which is smaller than the total size of the state space of 1820. Importantly, the dispersion of the calculated dependencies averaged over different samples is almost insensitive to the number of the bitstrings in the sample. However, as it was shown above

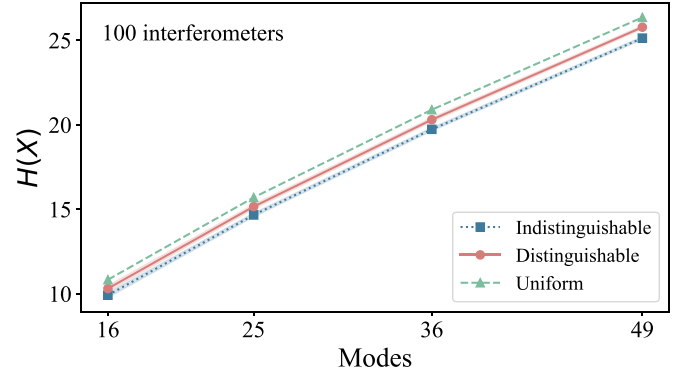


FIG. 7. Shannon entropy of probability distributions calculated for boson samplers with distinguishable (red solid line) and indistinguishable (blue dotted line) photons. The green dashed line denotes the case of the uniform sampler. The data were averaged over 100 boson samplers with different scattering matrices.

the averaging over different U matrices leads to a strong overlap of the unique degrees calculated with distinguishable and indistinguishable outcomes, which prevents us from using such a measure for certifying BS in an unsupervised manner.

The third measure to characterize BS complexity we develop in this work is aimed at quantifying information content produced by a boson sampler. It requires the account of the outcomes' probabilities, which means that *we go beyond the consideration above and remove the restrictions on the total number of measurements and the repetitions of the bitstrings*. However, the measurement outcomes are still considered to be collision free. Naturally, the first candidate to describe the information aspect of the BS complexity is the Shannon entropy, $H(X) = -\sum_x p_x \log_2 p_x$, where p_x is the probability of generating a particular bitstring x (here X denotes a random variable of obtained bitstring). The Shannon entropy estimates the optimal compression of data [53] that may be achieved for a given source. The obtained results (Fig. 7) show that the Shannon entropy is scaled linearly with respect to the number of output modes. For each BS setting the value of $H(X)$ calculated with the uniform sampler probabilities is nothing but the logarithm of the corresponding state space size. Unfortunately, a weak difference between the Shannon entropies calculated with probability distributions of distinguishable and indistinguishable photons motivates us to look for another informational measure.

In this situation, we propose first imitating the BS outcomes with a quantum state that can be initialized on a quantum computer or a quantum simulator. Upon measurements, such a state should reproduce the bitstring statistics of the collision-free boson sampler. It allows us to use the entire arsenal of quantum information theory measures to characterize such a wave function, and as we will show below, to quantify the difference between distinguishable and indistinguishable photons' sources.

At the level of outcomes a collision-free boson sampler can be imitated by using a system of quantum bits whose state in σ^z basis is characterized by a special structure of the basis wave functions. More specifically, the number of "1" in each

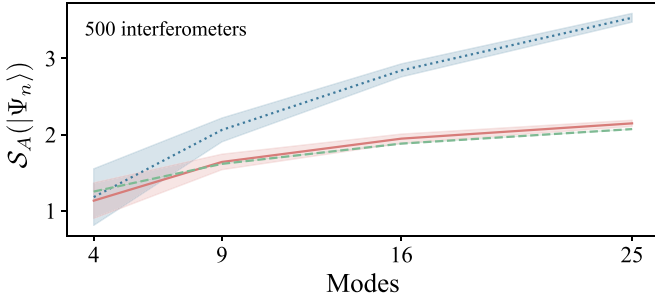


FIG. 8. Calculated von Neumann entropy for the quantum states that upon projective measurements imitate collision-free outcomes of boson samplers with distinguishable (red solid line) and indistinguishable (blue dotted line) photons. The data were averaged over 500 boson samplers with different scattering matrices. The green dashed line denotes the uniform sampler results.

basis vector with nonzero probability is fixed to the number of bosons n , while the total number of qubits is equal to the number of output modes m . In analogy to the notable Dicke states [54], one can write a random counterpart of such a quantum state as

$$|\Psi_n\rangle = \sum_j \alpha_j \mathcal{P}_j(|0\rangle^{\otimes m-n} \otimes |1\rangle^{\otimes n}), \quad (1)$$

where the sum goes over all possible permutations, \mathcal{P}_j of qubits, α_j is the amplitude of the j th basis function.

We would like to stress that Ψ_n is not the actual wave function of the boson sampler that should contain information about the complex scattering matrices [23] describing the internal structure of the device. In our case, we aim to reproduce only the BS outcomes having collision-free statistics with such a quantum state. It means that we have an infinite number of choices when defining the coefficients α_j in the wave function Eq. (1) that, in the general case, is a complex number with the only constraint $|\alpha_j|^2 = p_j$, where p_j is the probability to generate j th bitstring with BS. To simplify the consideration we take $\alpha_j = \sqrt{p_j}$ to be a real-valued coefficient. As for the particular complexity measure we choose von Neumann entropy $\mathcal{S}_A(|\Psi_n\rangle) = -\text{Tr}[\rho_A \log_2 \rho_A]$, where $\rho_A = \text{Tr}_B |\Psi_n\rangle \langle \Psi_n|$ is the reduced density matrix for a half-system bipartition into regions A and B .

In Fig. 8 we compare the von Neumann entropies calculated in the case of wave functions imitating outcomes of boson samplers with uniform, distinguishable, and indistinguishable particles. In the case of $m \geq 9$ the averaged data that corresponds to the measure \mathcal{S}_A for indistinguishable particles are well separated from others, which allows us to discriminate this source. The wave functions Ψ_n corresponding to the distinguishable and uniform device outcomes are featured with a saturation of the entropy value of around two bits. At the same time the quantum state that reproduces indistinguishable outcomes demonstrates a permanent growth as the number of modes increases. Remarkably, averaging of these results over 500 boson samplers with distinct scattering matrices is characterized by the standard deviation that decreases with increasing the mode's number, which paves another way to the accurate classification of unknown boson sampling devices.

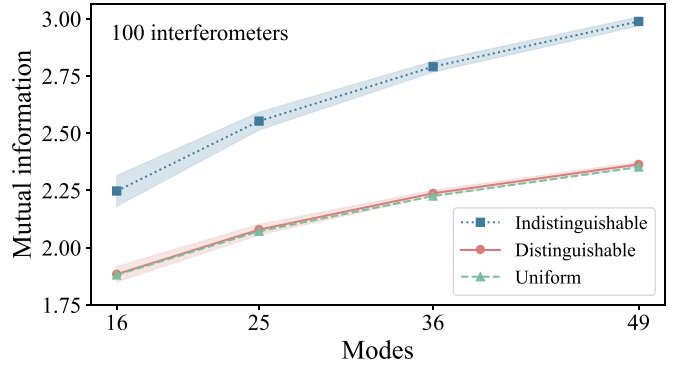


FIG. 9. Classical mutual information between two groups of output modes $1, \dots, \lceil m/2 \rceil$ and $\lceil m/2 \rceil + 1, \dots, m$ for boson samplers with distinguishable (red solid line) and indistinguishable (blue dotted line) photons. The green dashed line denotes the case of uniform sampler. The data were averaged over 100 boson samplers with different scattering matrices.

In general case, constructing the quantum state that imitates BS outcomes assumes accumulation of the considerable amount of bitstrings whose number should be enough to restore the probabilities of the basis functions. Then one needs to initialize the quantum state with the particular amplitudes. Thus, the practical realization of the third complexity measure is related to quantum-state tomography problem, which is characterized by considerable limitations on the number of qubits in the system in question. However, as it was shown in Ref. [55], implementation of the neural network quantum states can facilitate the solution of the tomography problem for some classes of wave functions, which suggests a distinct way for constructing such entanglement-based BS testers.

One can also note that the von Neumann entropy $\mathcal{S}_A(|\Psi_n\rangle)$ actually provides a half of the value of the quantum mutual information

$$\mathcal{I}(A : B) = \mathcal{S}_A(|\Psi_n\rangle) + \mathcal{S}_B(|\Psi_n\rangle) - \mathcal{S}(|\Psi_n\rangle) = 2\mathcal{S}_A(|\Psi_n\rangle) \quad (2)$$

between mode groups A and B . Here $\mathcal{S}_B(|\Psi_n\rangle)$ and $\mathcal{S}(|\Psi_n\rangle) = 0$ are von Neumann entropies of modes group B and whole pure state $|\Psi_n\rangle$, correspondingly. In Fig. 9 we illustrate the behavior of the corresponding classical mutual information

$$J(A:B) = H(A) + H(B) - H(X), \quad (3)$$

where $H(A)$ and $H(B)$ are Shannon entropies of the bitstrings' output at mode groups A and B , correspondingly. One can see that the values of the classical mutual information drastically differ for indistinguishable and distinguishable photons. At the same time, the classical mutual information for distinguishable photons is almost the same for the uniform distribution. Thus, the behavior of the classical mutual information agrees qualitatively with that calculated on the basis of von Neumann entropy in the quantum case.

III. CONCLUSION AND OUTLOOK

In this paper, we develop the procedure for benchmarking boson samplers and distinguishing different regimes of

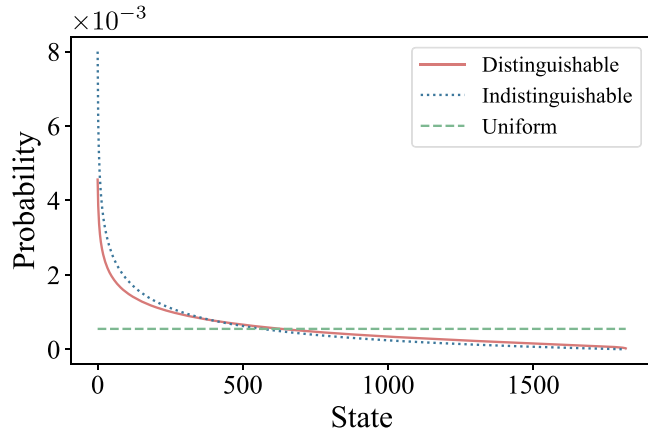


FIG. 10. Average sorted profiles for distinguishable (red solid line) and indistinguishable (blue dotted line) regimes of boson sampler with four photons and 16 output modes. Probability corresponding to uniform distribution is denoted as green dashed line for reference.

the multiphoton interference using network theory. Our approach is based on constructing networks for limited number of collision- and repetition-free BS outcomes by using the Hamming distances as a parameter that controls the net structure. Already at this level it becomes possible to distinguish uniform and nonuniform BS devices by comparing the degree distributions of the constructed networks. In turn, the certification of the nonuniform samplers into distinguishable or indistinguishable classes is shown to be a more delicate problem that can be solved with machine learning. The performed ML calculations reveal a high accuracy ($>98\%$) in classifying distinguishable and indistinguishable photon sources. Importantly, the number of the bitstrings required for such an accurate classification in the considered settings changes slightly as the number of output modes increases while there is an exponential growth of the state space size.

The proposed scheme for benchmarking boson samplers is mainly based on the information about unique degrees of the constructed networks. At the same time, network links can have different weights depending on the particular values of the Hamming distance between outcomes. Taking this into account would enrich and extend the characterization of boson samplers by using network theory. However, benchmarking with machine learning could also benefit from considering the weights since it could produce distinct useful features.

Ignoring the collision events in the BS data allows us to explore a connection between BS sampling and quantum computing. Namely, we derive and characterize random Dicke wave functions that reproduce the statistics over BS outcomes for distinguishable and indistinguishable sources. These quantum states reveal different behavior in the entanglement depending on the system size. Thus, a distinct research line can be initiated to explore ways, including the approximation of the wave function with neural network for efficient reconstructing of random Dicke states on a quantum device.

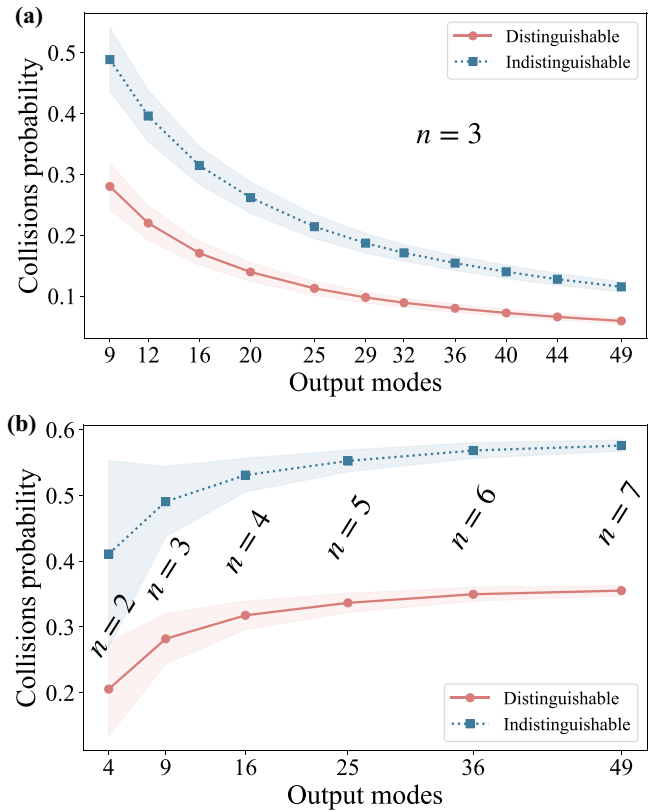


FIG. 11. Overall probability of generating outcome with collisions. (a) Results obtained with fixed number of bosons, $n = 3$ and different numbers of output modes. (b) The number of bosons and output modes are varied as $n = \sqrt{m}$, where m is the number of output modes. The data for each setting were averaged over 1000 scattering matrices. Colored regions denote the corresponding standard deviations.

From the perspective of the real BS experiments, exploration of the intermediate regimes between limits of indistinguishable and distinguishable particles that are purely theoretical is of a particular interest for further development of the Hamming network approach. In this regard, one can combine the proposed machine learning scheme with numerical methods for simulating the photon of a partial distinguishability [56,57]. Thus, the ML models trained in this work can be examined on the samples with predefined degrees of distinguishability. However, such degrees can themselves be used as labels in machine learning, which assumes the classification with respect to more than two classes, as was done in this work. All these steps will facilitate implementation of our approach in diagnosing real BS devices.

ACKNOWLEDGMENTS

This work was supported by the Russian Roadmap on Quantum Computing (Contract No. 868-1.3-15/15-2021, October 5, 2021). The work of AKF is also supported by the RSF Grant No. 19-71-10092 (analysis of certain aspects of machine learning applications).

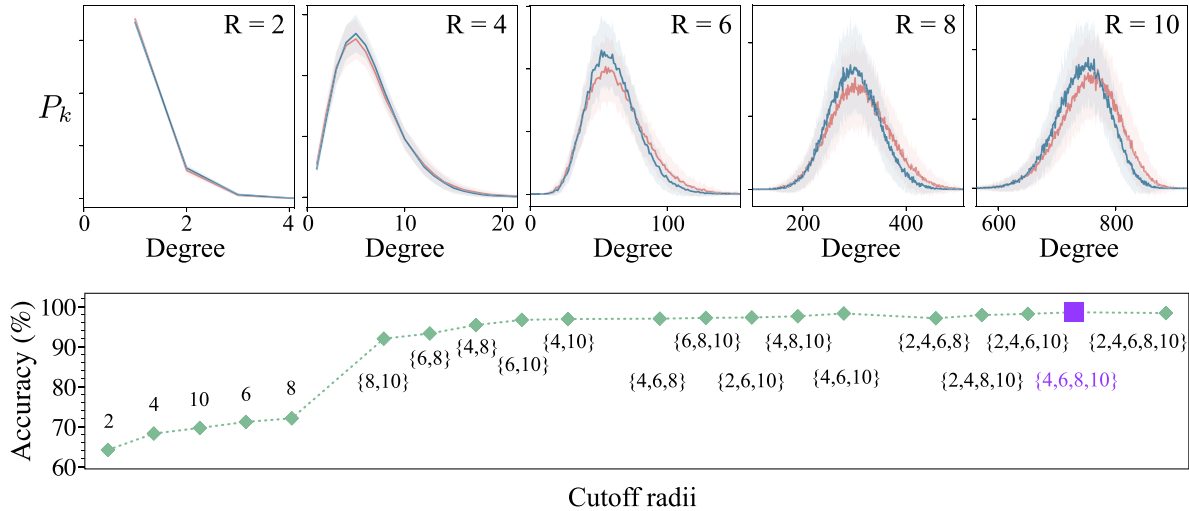


FIG. 12. (Top) Comparison of the averaged distributions for indistinguishable (blue upper line) and distinguishable (red lower line) bosons, obtained at different cutoff radii using $N = 1024$ unique bitstrings from a boson sampler with $n = 6$ and $m = 36$. All the results are averaged over 100 random U matrices. (Bottom) Accuracy dependence on the cutoff radii used to define feature vector. The best accuracy is marked with purple square and equal to 98.9%.

APPENDIX A: BOSON SAMPLING

In this work we used the BOSON-SAMPLING PYTHON package [58] to calculate the probability distributions for a given boson sampler matrix U that is an $m \times n$ matrix that describe a relation between the creation operators of input (\hat{a}_i^\dagger) and output (\hat{b}_i^\dagger) modes. The Haar-distributed complex unitary interferometer matrix itself was generated by using the STRAWBERRY FIELDS PYTHON package [59,60], which utilizes the classical groups approach [61]. In Fig. 10 we compare the sorted probability distributions for collision-free outcomes obtained from distinguishable, indistinguishable, and uniform boson samplers. One can see that there is little difference between the profiles obtained with distinguishable and indistinguishable particles, which clearly demonstrates the complexity of the source benchmarking with a limited number of outcomes. In general, to reproduce these probability profiles by using the statistics of the outcomes, the number of bitstrings should be four or five times larger than the size of the state space.

Detecting the collision events in the real experiments represents a significant technological challenge, which makes selecting the collision-free outcomes a natural solution when benchmarking a BS device. Since neglecting collision events leads to considerable changes in the behavior of the correlation-based features, as was demonstrated in Figs. 4(c) and 4(d) in the main text, it is important to estimate the probabilities of generating an event with collisions in different BS settings. For instance, in Fig. 11(a) we show such a collision outcome probability as a function of the number of output modes at a fixed number of bosons. As one would expect, the probability decays quickly as m increases.

The situation is completely different if the number of output modes depends on the number of bosons as $m = n^2$ [Fig. 11(b)], which can be associated to the lower bound for demonstrating quantum advantage. In this case the collision probability for indistinguishable particles does not decreases

with m . Instead it is saturated at a rather high value of about 0.55, which suggests a careful examination of the results of the previous correlation-function-based studies [23,50] when applying them for analysis of real experiments. Another important finding is that the collision probability for distinguishable particles is about two times smaller than that for indistinguishable ones. This means that the initial assumption about the distinguishability of photons can be made based on the amount of samples required to get N bitstrings without collisions. However, when analyzing the experimental data, one should also keep in mind the loss of photons and the precision of the detectors used.

In contrast to the collisions, the amount of repetitions drastically decreases with n . As can be seen from Table I, bitstrings collected from BS with $n \geq 6$ are almost unique up to some moderate number N . This is obviously connected with the rapid growth of the state space. Thus, excluding repetitions plays a role only when considering the $n = 4$ sampler.

TABLE I. Percentage of repetitions $(N_{\text{meas}} - N)/N_{\text{meas}}$, (%) in the N_{meas} outcomes with N unique bitstrings. The results are averaged over 100 random U matrices.

N	n	Distinguishable	Indistinguishable
512	4	27.715	37.419
	5	1.019	1.605
	6	0.018	0.057
	7	0.0	0.002
1024	4	54.045	67.680
	5	1.957	3.322
	6	0.055	0.095
	7	0.002	0.001

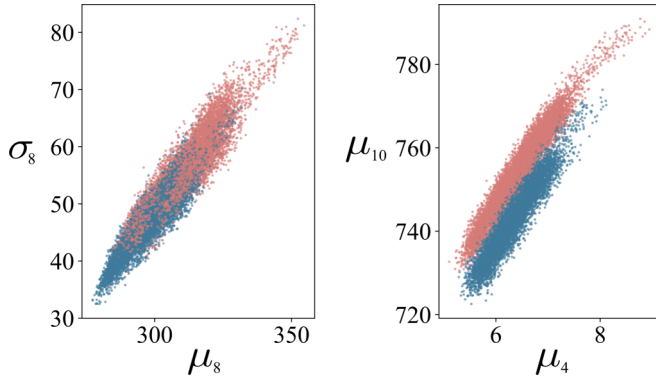


FIG. 13. Low-dimensional visualizations of the configurations taken from the training sets for $n = 6$ bosons and $m = 36$ output modes, $N = 1024$. Red (light gray) and blue (dark gray) clouds correspond to distinguishable and indistinguishable particles, respectively. Features were taken from the Hamming networks providing the best possible accuracy on a single R (left) and pair of cutoff radii (right). Namely, $R = 8$ and $R = \{4, 10\}$.

APPENDIX B: CHOICE OF THE CUTOFF RADII

In this section we discuss the choice of the cutoff radius when constructing Hamming nets. As was shown in Ref. [13] one should avoid overcounting isolated nodes and keep a nontrivial network structure. Undoubtedly, such a choice is problem-specific and in our study we are looking for the R values at which properties of the distinguishable network differs as much as possible from that obtained with indistinguishable bosons. We calculate the degree distribution that defines a fraction of nodes with k connections to other nodes and it is standard measure to characterize a graph or network. We find out that the most reliable features are the two first moments of the P_k distributions for such intermediate cutoff radii for which P_k is Gaussian-like and has both left and right sides.

Importantly, taking into account distributions at small R may also be useful since the mean values of P_k distributions are rather robust and then it gives some new dimensions to the feature space where there is at least some discrepancy between the different BS regimes. However, as can be seen from Fig. 12, this is not the case if we already took into account all the meaningful cutoff radii. Thus, we use $R = \{2, 4, 6\}$, $R = \{2, 4, 6, 8\}$, $R = \{4, 6, 8, 10\}$, and $R = \{6, 8, 10, 12\}$ for the samplers with $n = 4, 5, 6$, and 7 photons, respectively.

The reason why the accuracy is low when taking into account the single cutoff radius is that the clouds formed by different samplers strongly overlap in the σ - μ plane. As can be seen from Fig. 13, adding at least one extra R leads to the formation of the almost-separated clouds in μ_1 - μ_2 plane. We should stress that both moments of P_k distributions are essential since it leads to better separation of the configurations in the higher-dimensional parameter space.

APPENDIX C: MACHINE LEARNING

To solve the problem of distinguishing between two different BS regimes we train several basic ML algorithms implemented in the SCIKIT-LEARN PYTHON package [62].

TABLE II. Comparison of the accuracy (%) of different ML classifiers trained with the same data set on the unseen U matrices. Features were taken from both Hamming network and mode-mode correlations.

N	n	LR	SVM	RF	k -NN
512	4	95.6(1)	94.3(1)	93.3(1)	93.0(1)
	5	97.1(1)	96.9(1)	96.4(1)	96.6(1)
	6	91.8(1)	91.6(1)	90.9(1)	90.7(1)
	7	89.0(1)	88.9(1)	88.6(1)	88.7(1)
1024	4	100.0	100.0	100.0	100.0
	5	99.8(1)	99.8(1)	99.7(1)	99.6(1)
	6	98.9(1)	98.8(1)	98.5(1)	98.6(1)
	7	98.3(1)	98.2(1)	98.2(1)	98.1(1)

Namely, a logistic regression (LR), a support vector machine (SVM), random forest (RF), and k -nearest neighbors (k -NN) classifiers. For LR we use the *liblinear* solver, for SVM (the radial basis function as a kernel and $\gamma = 1/N_f$, where N_f is the length of our feature vector), and for RF 300 estimators. The amount of nearest neighbors in k -NN we adjust manually for each data set to obtain the best accuracy. The rest of the parameters of the algorithms were chosen to be the default ones.

The main data set includes 100 samples for each regime for each of 80 different U matrices. We randomly shuffle these data and use 80% as a training set and 20% as a testing one. To check the accuracy on the unseen data we generate and use an additional 4000 samples from 20 completely new random U matrices. Since each feature lies in its own range and has its own dispersion, additional standardization is done on the basis of the training samples.

As can be seen from Table II, all the presented algorithms show similar performance on the unseen data when we use features taken from both the Hamming network and mode-mode correlations. However, LR is more stable, faster, and slightly outperforms the rest in most cases which makes it more preferable for the analysis of the currently available interferometers.

It is important to note that the trainability of the ML algorithms used for the discrimination in general does not depend on n since the structure of the input feature vector is constant. However, the features themselves, i.e., the first two moments of the P_k distributions and the distribution of the mode-mode correlations, depend on the ratio N/C_m^n , where n is the number of photons and m is the number of the output modes. Therefore, we expect that the differences between the distinguishable and indistinguishable photons on the level of features will become less significant if we fix N and increase n further. Thus, the increase of n will definitely lead to the decrease of the accuracy, and at some point, to the inability of accessing the same precision under experimentally achievable conditions. However, since we are dealing with the ML algorithms, one cannot preliminary assess to what extent these changes will affect the results. Nevertheless, the results presented in the paper demonstrate that the proposed approach is potentially applicable for the analysis of the currently available state-of-the-art BS.

- [1] G. Brassard, I. Chuang, S. Lloyd, and C. Monroe, Quantum computing, *Proc. Natl. Acad. Sci.* **95**, 11032 (1998).
- [2] T. D. Ladd, F. Jelezko, R. Laflamme, Y. Nakamura, C. Monroe, and J. L. O'Brien, Quantum computers, *Nature (London)* **464**, 45 (2010).
- [3] A. K. Fedorov, N. Gisin, S. M. Belousov, and A. I. Lvovsky, Quantum computing at the quantum advantage threshold: A down-to-business review, [arXiv:2203.17181](https://arxiv.org/abs/2203.17181).
- [4] P. W. Shor, Algorithms for quantum computation: Discrete logarithms and factoring, in *Proceedings 35th Annual Symposium on Foundations of Computer Science (IEEE, Washington, D.C., 1994)*, pp. 124–134.
- [5] F. Arute *et al.*, Quantum supremacy using a programmable superconducting processor, *Nature (London)* **574**, 505 (2019).
- [6] E. Pednault, J. A. Gunnels, G. Nannicini, L. Horesh, and R. Wisnieff, Leveraging secondary storage to simulate deep 54-qubit sycamore circuits, [arXiv:1910.09534](https://arxiv.org/abs/1910.09534).
- [7] C. Huang *et al.*, Classical simulation of quantum supremacy circuits, [arXiv:2005.06787](https://arxiv.org/abs/2005.06787).
- [8] F. Pan and P. Zhang, Simulation of quantum circuits using the big-batch tensor network method, *Phys. Rev. Lett.* **128**, 030501 (2022).
- [9] D. Aharonov, X. Gao, Z. Landau, Y. Liu, and U. Vazirani, A polynomial-time classical algorithm for noisy random circuit sampling, in *Proceedings of the 55th Annual ACM Symposium on Theory of Computing, STOC 2023 (Association for Computing Machinery, New York, 2023)*, pp. 945–957.
- [10] M. Liu, J. Liu, Y. Alexeev, and L. Jiang, Estimating the randomness of quantum circuit ensembles up to 50 qubits, *npj Quantum Inf.* **8**, 137 (2022).
- [11] J. C. Napp, R. L. La Placa, A. M. Dalzell, F. G. S. L. Brandão, and A. W. Harrow, Efficient classical simulation of random shallow 2D quantum circuits, *Phys. Rev. X* **12**, 021021 (2022).
- [12] O. M. Sotnikov, I. A. Iakovlev, A. A. Iliasov, M. I. Katsnelson, A. A. Bagrov, and V. V. Mazurenko, Certification of quantum states with hidden structure of their bitstrings, *npj Quantum Inf.* **8**, 41 (2022).
- [13] T. Mendes-Santos *et al.*, Wave function network description and kolmogorov complexity of quantum many-body systems, [arXiv:2301.13216](https://arxiv.org/abs/2301.13216).
- [14] A. Morvan *et al.*, Phase transition in random circuit sampling, [arXiv:2304.11119](https://arxiv.org/abs/2304.11119).
- [15] S. Aaronson and A. Arkhipov, The computational complexity of linear optics, *Theory of Computing* **9**, 143 (2013).
- [16] C. Gogolin, M. Kliesch, L. Aolita, and J. Eisert, Boson-sampling in the light of sample complexity, [arXiv:1306.3995](https://arxiv.org/abs/1306.3995).
- [17] M. C. Tichy, Interference of identical particles from entanglement to boson-sampling, *J. Phys. B: At., Mol. Opt. Phys.* **47**, 103001 (2014).
- [18] D. J. Brod, E. F. Galvão, A. Crespi, R. Osellame, N. Spagnolo, and F. Sciarrino, Photonic implementation of boson sampling: A review, *Adv. Photonics* **1**, 034001 (2019).
- [19] M. Tillmann, B. Dakić, R. Heilmann, S. Nolte, A. Szameit, and P. Walther, Experimental boson sampling, *Nat. Photonics* **7**, 540 (2013).
- [20] M. A. Broome, A. Fedrizzi, S. Rahimi-Keshari, J. Dove, S. Aaronson, T. C. Ralph, and A. G. White, Photonic boson sampling in a tunable circuit, *Science* **339**, 794 (2013).
- [21] J. B. Spring *et al.*, Boson sampling on a photonic chip, *Science* **339**, 798 (2013).
- [22] S.-T. Wang and L.-M. Duan, Certification of boson sampling devices with coarse-grained measurements, [arXiv:1601.02627](https://arxiv.org/abs/1601.02627).
- [23] M. Walschaers, J. Kuipers, J.-D. Urbina, K. Mayer, M. C. Tichy, K. Richter, and A. Buchleitner, Statistical benchmark for bosonsampling, *New J. Phys.* **18**, 032001 (2016).
- [24] H.-L. Huang, H.-S. Zhong, T. Li, F.-G. Li, X.-Q. Fu, S. Zhang, X. Wang, and W.-S. Bao, Statistical analysis for collision-free boson sampling, *Sci. Rep.* **7**, 15265 (2017).
- [25] U. Chabaud, F. Grosshans, E. Kashefi, and D. Markham, Efficient verification of Boson Sampling, *Quantum* **5**, 578 (2021).
- [26] E.-J. Kuo, Y. Xu, D. Hangleiter, A. Grankin, and M. Hafezi, Boson sampling for generalized bosons, *Phys. Rev. Res.* **4**, 043096 (2022).
- [27] A. S. Popova and A. N. Rubtsov, Cracking the quantum advantage threshold for Gaussian boson sampling, [arXiv:2106.01445](https://arxiv.org/abs/2106.01445).
- [28] B. Villalonga, M. Y. Niu, L. Li, H. Neven, J. C. Platt, V. N. Smelyanskiy, and S. Boixo, Efficient approximation of experimental gaussian boson sampling, [arXiv:2109.11525](https://arxiv.org/abs/2109.11525).
- [29] H.-S. Zhong *et al.*, Quantum computational advantage using photons, *Science* **370**, 1460 (2020).
- [30] H.-S. Zhong *et al.*, Phase-programmable gaussian boson sampling using stimulated squeezed light, *Phys. Rev. Lett.* **127**, 180502 (2021).
- [31] L. S. Madsen *et al.*, Quantum computational advantage with a programmable photonic processor, *Nature (London)* **606**, 75 (2022).
- [32] Y.-H. Deng *et al.*, Gaussian boson sampling with pseudo-photon-number-resolving detectors and quantum computational advantage, *Phys. Rev. Lett.* **131**, 150601 (2023).
- [33] N. Spagnolo *et al.*, Experimental validation of photonic boson sampling, *Nat. Photonics* **8**, 615 (2014).
- [34] H. Wang *et al.*, Boson sampling with 20 input photons and a 60-mode interferometer in a 10^{14} -dimensional hilbert space, *Phys. Rev. Lett.* **123**, 250503 (2019).
- [35] B. Seron, L. Novo, A. Arkhipov, and N. J. Cerf, Efficient validation of boson sampling from binned photon-number distributions, [arXiv:2212.09643](https://arxiv.org/abs/2212.09643).
- [36] L. Pioge, B. Seron, L. Novo, and N. J. Cerf, Enhanced bunching of nearly indistinguishable bosons, [arXiv:2308.12226](https://arxiv.org/abs/2308.12226).
- [37] I. Agresti, N. Viggianiello, F. Flamini, N. Spagnolo, A. Crespi, R. Osellame, N. Wiebe, and F. Sciarrino, Pattern recognition techniques for boson sampling validation, *Phys. Rev. X* **9**, 011013 (2019).
- [38] Y.-H. Luo *et al.*, Quantum teleportation in high dimensions, *Phys. Rev. Lett.* **123**, 070505 (2019).
- [39] T. Giordani, V. Mannucci, N. Spagnolo, M. Fumero, A. Rampini, E. Rodolà, and F. Sciarrino, Certification of gaussian boson sampling via graphs feature vectors and kernels, *Quantum Sci. Technol.* **8**, 015005 (2023).
- [40] F. Flamini, N. Spagnolo, and F. Sciarrino, Visual assessment of multi-photon interference, *Quantum Sci. Technol.* **4**, 024008 (2019).
- [41] H. Wang *et al.*, High-efficiency multiphoton boson sampling, *Nat. Photonics* **11**, 361 (2017).
- [42] H.-S. Zhong *et al.*, 12-photon entanglement and scalable scattershot boson sampling with optimal entangled-photon pairs from parametric down-conversion, *Phys. Rev. Lett.* **121**, 250505 (2018).
- [43] S. Aaronson and A. Arkhipov, Bosonsampling is far from uniform, *Quantum Inf. Comput.* **14**, 1383 (2014).

- [44] N. Granik, L. E. Weiss, E. Nehme, M. Levin, M. Chein, E. Perlson, Y. Roichman, and Y. Shechtman, Single-particle diffusion characterization by deep learning, *Biophys. J.* **117**, 185 (2019).
- [45] I. A. Iakovlev, A. Y. Deviatov, Y. Lvov, G. Fakhruullina, R. F. Fakhruullin, and V. V. Mazurenko, Probing diffusive dynamics of natural tubule nanoclays with machine learning, *ACS Nano* **16**, 5867 (2022).
- [46] J. Carrasquilla and R. G. Melko, Machine learning phases of matter, *Nat. Phys.* **13**, 431 (2017).
- [47] I. A. Iakovlev, O. M. Sotnikov, and V. V. Mazurenko, Profile approach for recognition of three-dimensional magnetic structures, *Phys. Rev. B* **99**, 024430 (2019).
- [48] O. M. Sotnikov and V. V. Mazurenko, Neural network agent playing spin hamiltonian games on a quantum computer, *J. Phys. A: Math. Theor.* **53**, 135303 (2020).
- [49] N. Jiang, Y. F. Pu, W. Chang, C. Li, S. Zhang, and L. M. Duan, Experimental realization of 105-qubit random access quantum memory, *npj Quantum Inf.* **5**, 28 (2019).
- [50] F. Flamini, M. Walschaers, N. Spagnolo, N. Wiebe, A. Buchleitner, and F. Sciarrino, Validating multi-photon quantum interference with finite data, *Quantum Sci. Technol.* **5**, 045005 (2020).
- [51] S. Lloyd, Measures of complexity: a nonexhaustive list, *IEEE Control Syst. Mag.* **21**, 7 (2001).
- [52] A. A. Bagrov, I. A. Iakovlev, A. A. Iliasov, M. I. Katsnelson, and V. V. Mazurenko, Multiscale structural complexity of natural patterns, *Proc. Natl. Acad. Sci.* **117**, 30241 (2020).
- [53] M. A. Nielsen and I. L. Chuang, *Quantum Computation and Quantum Information* (Cambridge University Press, Cambridge, England, 2000).
- [54] R. H. Dicke, Coherence in spontaneous radiation processes, *Phys. Rev.* **93**, 99 (1954).
- [55] G. Torlai, G. Mazzola, J. Carrasquilla, M. Troyer, R. Melko, and G. Carleo, Neural-network quantum state tomography, *Nat. Phys.* **14**, 447 (2018).
- [56] J. J. Renema, A. Menssen, W. R. Clements, G. Triginer, W. S. Kolthammer, and I. A. Walmsley, Efficient classical algorithm for boson sampling with partially distinguishable photons, *Phys. Rev. Lett.* **120**, 220502 (2018).
- [57] M. C. Tichy, Sampling of partially distinguishable bosons and the relation to the multidimensional permanent, *Phys. Rev. A* **91**, 022316 (2015).
- [58] IffTech and J. Long, Boson-sampling, <https://github.com/IffTech/Boson-Sampling>.
- [59] T. R. Bromley, J. M. Arrazola, S. Jahangiri, J. Izaac, N. Quesada, A. D. Gran, M. Schuld, J. Swinerton, Z. Zabaneh, and N. Killoran, Applications of near-term photonic quantum computers: Software and algorithms, *Quantum Sci. Technol.* **5**, 034010 (2020).
- [60] N. Killoran, J. Izaac, N. Quesada, V. Bergholm, M. Amy, and C. Weedbrook, Strawberry Fields: A Software Platform for Photonic Quantum Computing, *Quantum* **3**, 129 (2019).
- [61] F. Mezzadri, How to generate random matrices from the classical compact groups, *NOTICES of the AMS*, **54**, 592 (2007).
- [62] F. Pedregosa *et al.*, Scikit-learn: Machine learning in Python, *Journal of Machine Learning Research* **12**, 2825 (2011).